

# Nature of crossover between localized and itinerant $5f$ states in $\text{URu}_2\text{Si}_2$ evidenced by $^{29}\text{Si}$ -NMR measurement

N. Emi,<sup>1</sup> R. Hamabata,<sup>1</sup> T. Koyama,<sup>1</sup> G. Motoyama,<sup>2</sup> K. Ueda,<sup>1</sup> T. Kohara,<sup>1</sup> and T. Mito<sup>1,\*</sup>

<sup>1</sup>*Graduate School of Material Science, University of Hyogo, Hyogo 678-1297, Japan*

<sup>2</sup>*Department of Materials Science, Shimane University, Shimane 690-8504, Japan*

(Received 6 June 2016; revised manuscript received 28 August 2017; published 7 November 2017)

We have carried out  $^{29}\text{Si}$  nuclear magnetic resonance of  $\text{URu}_2\text{Si}_2$ , which undergoes the so-called hidden order (HO) at  $T_{\text{HO}} = 17.5$  K. The use of a  $^{29}\text{Si}$ -enriched sample enabled us to obtain accurate NMR data up to 350 K and to extract the features of low energy magnetic correlations at high temperatures in this compound. Present results naturally indicate that  $\text{URu}_2\text{Si}_2$  undergoes a crossover from localized to itinerant regimes with decreasing temperature and the HO occurs in the crossover region. We also discuss possible antiferromagnetic correlations remaining down to  $T_{\text{HO}}$  by extracting magnetic fluctuation components.

DOI: [10.1103/PhysRevB.96.195113](https://doi.org/10.1103/PhysRevB.96.195113)

Two contrary characteristics of  $f$  electrons in compounds, namely itinerant and localized ones, bring a variety of intriguing properties depending on the sort of electronic correlations. The uranium compound  $\text{URu}_2\text{Si}_2$  has been regarded as one of the prototypes showing the two characteristics [1] and attracting much interest since its discovery 30 years ago [2–4]. This compound undergoes the phase transition called hidden order (HO) at  $T_{\text{HO}} = 17.5$  K as well as the superconducting transition at  $T_c = 1.4$  K. Despite a large jump of the specific heat at  $T_{\text{HO}}$ , suggesting an intimate relationship between heavy quasiparticles and the HO, the degrees of freedom responsible for the transition have not been identified. The itinerant-localized duality, characteristic of the U compounds, may increase the complexity of the HO problem. It is therefore indispensable to identify the properties of  $5f$  electrons for  $T > T_{\text{HO}}$  where underlying correlations giving rise to the HO possibly develop as temperature approaches  $T_{\text{HO}}$ .

Nuclear magnetic resonance (NMR) is one of the powerful tools to investigate the electronic states in terms of low-energy magnetic correlations. Indeed, there are several NMR studies on the problems of the HO [5–13] and the superconductivity [5,6]. However, surprisingly, the detailed measurements in the high-temperature region of  $\text{URu}_2\text{Si}_2$  have not been reported so far. Consequently, the issue of whether the HO occurs in the itinerant regime or the localized one has not been identified at least by the NMR study. This may be because the weak signal intensity of  $^{29}\text{Si}$ -NMR, arising from the low natural abundance of isotope  $^{29}\text{Si}$  ( $\sim 4.7\%$ ), prevents one from accomplishing accurate measurements at high temperatures.

To overcome the problem, we prepared a  $^{29}\text{Si}$ -enriched sample, which is useful to enhance the signal intensity drastically. Our results are naturally accounted for within a general phenomenon often seen in heavy fermion materials:  $\text{URu}_2\text{Si}_2$  undergoes a crossover from localized to itinerant regimes with decreasing temperature and the HO occurs just below a characteristic temperature of the crossover. Here, a remaining problem is whether or not all magnetic correlations are uniformly suppressed below the crossover temperature through the onset of coherence toward the Kondo lattice state.

In order to deduce electronic correlations possibly associated with the HO, we extracted magnetic fluctuation components parallel and perpendicular to the crystal  $c$  axis and found a possibility of remaining antiferromagnetic correlations just above  $T_{\text{HO}}$ .

A polycrystalline sample was synthesized by arc-melting constituent elements, including 93% enriched  $^{29}\text{Si}$ , together in an argon atmosphere. The ingot was annealed at  $980^\circ\text{C}$  for two weeks before it was powdered. The powdered sample was oriented in a magnetic field  $H$  (i.e., the tetragonal  $c$  axis is parallel to  $H$ ) by using the strongly anisotropic magnetization of this compound, and Knight shift  $K$  and nuclear spin lattice relaxation rate  $1/T_1$  for  $H \parallel c$  were measured up to 250 K. After those measurements, Stycast 1266 epoxy was added to the sample in field to fix the orientation, and then  $K$  and  $T_1$  for  $H \parallel c$  and  $H \perp c$  were measured up to 350 K. The degree of the orientation of the Stycast-mixed powder sample was checked by measuring the susceptibility. The susceptibility for  $H \perp c$  was well reproduced by assuming the mixture of a 2%  $H \parallel c$  component [see Fig. 7 in Ref. [14]]. This small  $H \parallel c$  component probably arises from the imperfect orientation of the powder sample. Note that neither any additional broadening nor shift in NMR lines was observed after the sample was mixed with Stycast [see Fig. 8 in Ref. [14]]. Also, in contrast to the above-mentioned macroscopic susceptibility measurement, we did not see any significant influence from the partial misorientation in the estimation of  $K$  and  $T_1$ , as described later. All the NMR experiments were carried out at the Si site (nuclear spin of  $^{29}\text{Si}$  nucleus is  $1/2$ ) using the spin-echo technique with a phase-coherent pulsed spectrometer in magnetic fields from 0.34–6.5 T. The magnetic field was calibrated using  $^{63}\text{Cu}$  of an NMR coil and  $^{27}\text{Al}$  as references: for the latter, we introduced a small amount of Al powder together with the  $\text{URu}_2\text{Si}_2$  sample into the NMR coil.  $T_1$  was measured by a single rf-pulse saturation method.

The use of the  $^{29}\text{Si}$ -enriched powdered sample produces NMR signal strong enough to obtain detailed NMR data up to the highest temperature of 350 K [representative spectra are shown in Fig. 1]. Note that the intensity of the NMR signal is roughly inversely proportional to temperature. However, the spectra below 10 K (not shown) are about twice as broad as that in the case of a single crystal sample [7,10]. This additional broadening may arise from local defects and/or the imperfect

\*mito@sci.u-hyogo.ac.jp

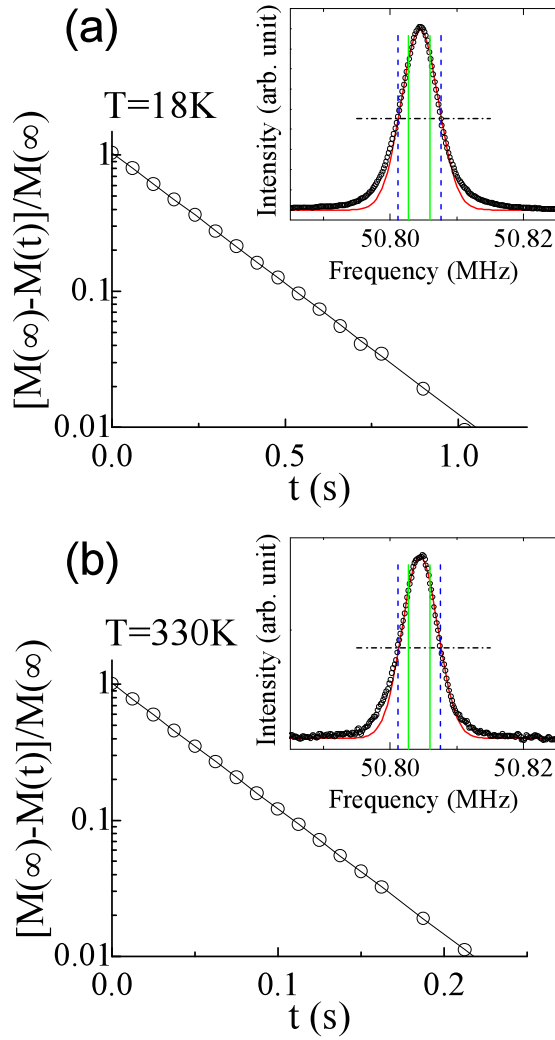


FIG. 1. Relaxation curves of  $^{29}\text{Si}$  nuclear magnetization measured at (a) 18 K and (b) 330 K and at  $H = 6.0$  T applied perpendicular to the  $c$  axis. The solid lines are fits of the data by  $[M(\infty) - M(t)]/M(\infty) = \exp(-t/T_1)$ . Insets show  $^{29}\text{Si}$ -NMR spectra obtained by Fourier-transforming the spin echo. The vertical broken (blue) and solid (green) lines indicate FWHM and  $1/2 \times \text{FWHM}$ , respectively. The nuclear magnetization was measured by integrating the signal between the solid lines. See text for details.

orientation of the powder sample mentioned above, which are inevitable when using a powder sample. In order to reduce the disadvantage, we estimated the Knight shift by fitting the spectra in a narrow region, namely within the full width at half maximum (FWHM) denoted by the vertical broken lines in the insets of Figs. 1(a) and 1(b) with a Gaussian function. For the  $T_1$  measurement, we integrated the signal between the  $1/2 \times \text{FWHM}$  lines, which are denoted by the vertical solid lines in the inset of Figs. 1(a) and 1(b) to evaluate the nuclear magnetization  $M$  at a delay  $t$  after a saturation pulse. As shown in Fig. 1, the  $T_1$  relaxation curve is excellently fitted by a single exponential function over the whole temperature range, indicating that the relaxation process is dominated by the inherent phase. We also note that consistency between NMR data on powder and single-crystal samples was confirmed

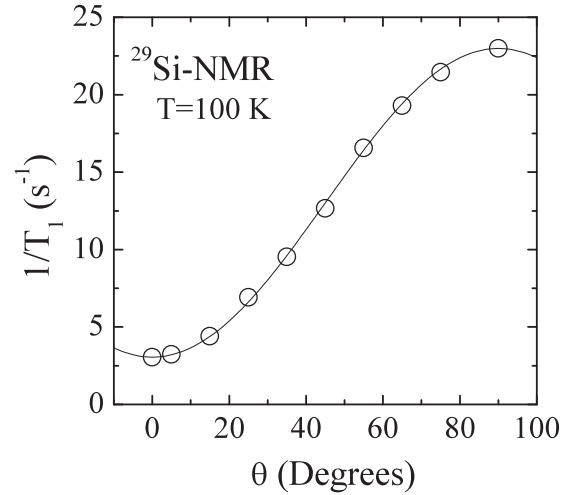


FIG. 2.  $\theta$  dependence of  $1/T_1$  measured at 100 K. The solid line indicates  $1/T_1(\theta) = (1/T_1)_{\parallel} \cos^2 \theta + (1/T_1)_{\perp} \sin^2 \theta$ .

by previous reports [see, for example, Ref. [11]]. Typical experimental errors in the present  $KT_1$ , and extracted data from them are smaller than the sizes of symbol in each figure.

The direction of the oriented sample was first set by eye and then checked by measuring  $T_1$  in magnetic field. Because of the sizable magnetic anisotropy in this compound,  $1/T_1$  also remarkably depends on  $\theta$ , an angle between the oriented  $c$  axis of the sample and  $H$ . As shown in Fig. 2, the  $\theta$  dependence is well reproduced as  $1/T_1(\theta) = (1/T_1)_{\parallel} \cos^2 \theta + (1/T_1)_{\perp} \sin^2 \theta$ , where  $(1/T_1)_{\parallel}$  and  $(1/T_1)_{\perp}$  are the nuclear spin relaxation rate for  $\theta = 0^\circ$  and  $90^\circ$ , respectively. Thus,  $\theta$  could be determined within an accuracy of  $\pm 3^\circ$ .

Figure 3(a) shows the temperature dependences of  $K$  for  $H \parallel c$  and  $H \perp c$ ,  $K_{\parallel}$  and  $K_{\perp}$ , respectively. In the low-temperature region below 30 K, the present  $K_{\parallel}$  is in excellent agreement with a precious study on a single crystalline sample [9].  $K_{\parallel}$  is largely enhanced compared to  $K_{\perp}$ , reflecting the Ising-like magnetic property.  $K_{\parallel}$  for  $T > 100$  K is well described by Curie-Weiss law, while  $K_{\perp}$  shows weak temperature dependence, in good agreement with the strong anisotropy in the bulk susceptibility [2]. In the present experiment, we found that  $K_{\perp}$  slightly increases with temperature above 100 K as shown in Fig. 3(b). Since we also find a linear relation between  $K_{\perp}$  and  $\chi_{\perp}$  [17] for  $90 < T < 290$  K [see the inset of Fig. 3(b) and Fig. 11 in Ref. [14]], this behavior is attributed not to the temperature variation in hyperfine coupling constant, but to the temperature dependence of the electronic susceptibility. The linear fit shown in the inset of Fig. 3(b) yields hyperfine coupling constant  $A_{\perp} = 3.82 \text{ kOe}/\mu_B$ . Compared to a hyperfine coupling constant for  $H \parallel c$ ,  $A_{\parallel} = 3.14 \text{ kOe}/\mu_B$ , we similarly obtained from a  $K_{\parallel}$  vs  $\chi_{\parallel}$  plot [see Fig. 11 of Ref. [14]].  $A_{\perp}/A_{\parallel} = 1.2$  reveals nearly isotropic characteristics of the hyperfine coupling constant, suggesting that the hyperfine field predominantly arises from Fermi contact interaction due to transferred  $U 5f$  moments to Si  $3s$  orbitals. The linear relation between  $K_{\perp}$  and  $\chi_{\perp}$  simultaneously reveals that the present estimation of  $K_{\perp}$  is not influenced by the partial misorientation

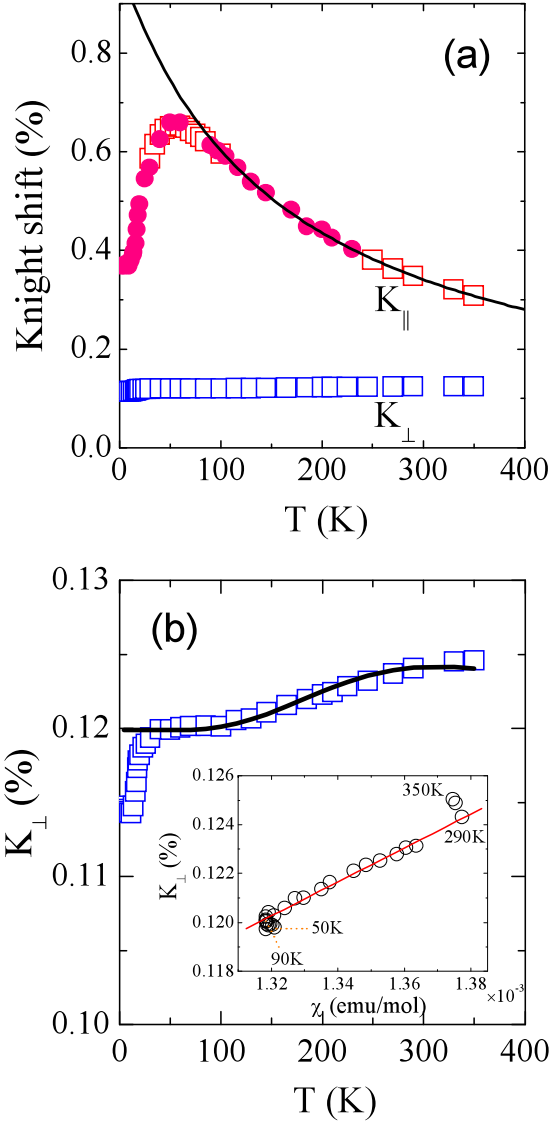


FIG. 3. (a) Temperature dependences of  $K_{\parallel}$  and  $K_{\perp}$ . We plot  $K_{\parallel}$  data taken before (solid circles) and after (open squares) the sample was mixed with Stycast to check the influence of Stycast. Magnetic fields for the former and latter measurements are  $H = 2.07$  and  $6.0$  T, respectively. The solid line shows Curie-Weiss fit to the data. (b) Expanded view of  $K_{\perp}$ . The solid line is the calculated temperature dependence of  $K_{\perp}$  within the CEF model. See text for details and Ref. [14]. Inset shows the plot of  $K_{\perp}$  vs  $\chi_{\perp}$  with temperature as an implicit variable. Here we adopted the  $\chi_{\perp}$  data reported by Galatanu *et al.* [17]. The solid line is a linear fit to the data.

of the powder sample mentioned before. We will discuss the temperature dependence of  $K_{\perp}$  later again.

The temperature dependence of  $1/T_1$  is another important clue to grasp the characteristics of  $5f$  electrons. As shown in Fig. 4(a),  $1/T_1$  for  $H \perp c$ ,  $(1/T_1)_{\perp}$ , is weakly dependent on temperature for  $100 < T < 200$  K and decreases with increasing temperature above 200 K. For well-localized  $f$  electron systems, where  $f$  electrons weakly interact with conduction electrons,  $1/T_1$  is decomposed into two contributions:  $(1/T_1)_c$  and  $(1/T_1)_f$ . The first term arises from interaction with the conduction electrons and depends linearly upon temperature

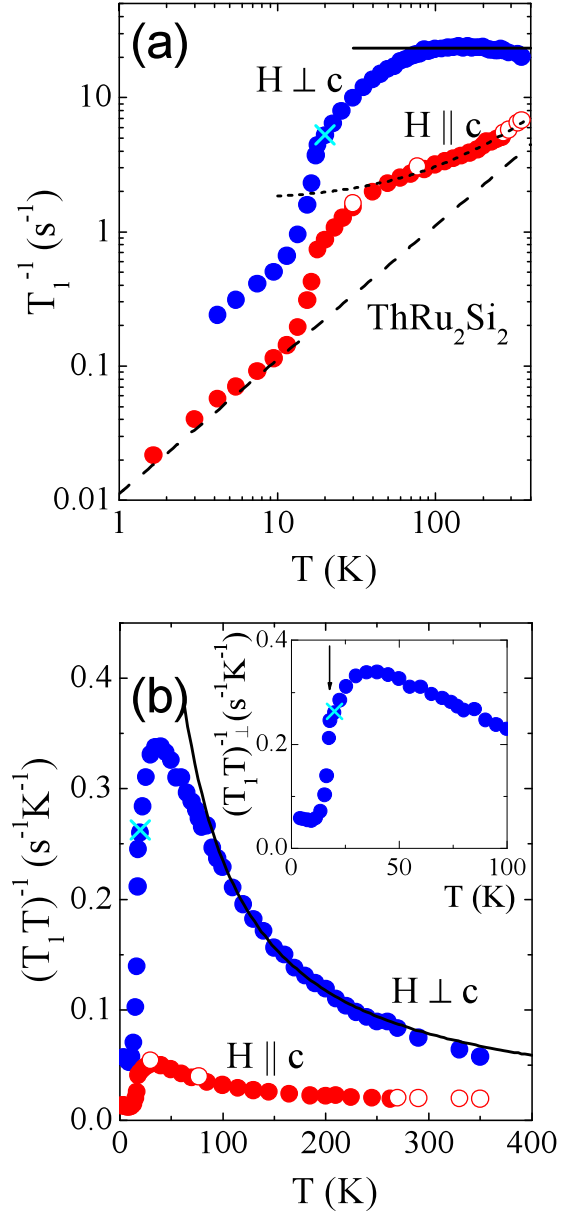


FIG. 4. (a) Temperature dependence of  $1/T_1$  for  $\text{URu}_2\text{Si}_2$  along with the temperature dependence for  $\text{ThRu}_2\text{Si}_2$  (broken line) [13]. For  $H \parallel c$ , we plot the data taken before (solid circles) and after (open circles) the sample was mixed with Stycast. At 20 K for  $H \perp c$ , we plot two  $1/T_1$  data measured at different fields 6.0 T (solid circle) and 0.34 T (cross), which are in good accordance with each other.  $1/T_1$  for  $\text{ThRu}_2\text{Si}_2$  is isotropic within experimental accuracy [13]. The solid line represents the temperature independent behavior of  $(1/T_1)_{\perp}$  for  $100 < T < 200$  K, and the dotted line does a least-squares fit of  $1/T_1 = aT + b$  to the data for  $T > 100$  K. See text for details. (b) Temperature dependence of  $1/T_1 T$  for  $\text{URu}_2\text{Si}_2$ . The solid line indicates Curie fit to the data for  $100 < T < 200$  K. The inset shows an expanded view of  $(1/T_1 T)_{\perp}$  for  $T < 100$  K. The arrow indicates  $T_{\text{HO}}$ .

(the so-called Korringa relation between the nucleus and the conduction electron). The second term  $(1/T_1)_f$  is the contribution of the  $f$  electrons, and when  $f$  electron moments are regarded as fluctuating independently, it is described as

$(1/T_1)_f \propto k_B T \chi \tau_f$  [18]. Here,  $k_B$  is the Boltzmann constant,  $\chi$  is the bulk susceptibility, and  $\tau_f$  is the effective correlations time of the local moments. Moreover,  $1/\tau_f$  predominantly consists of two terms:  $1/\tau_{ff}$  and  $1/\tau_{cf}$  [19].  $1/\tau_{ff}$  originates from exchange interaction between  $f$  electrons through the Ruderman-Kittel-Kasuya-Yosida (RKKY) interaction and is considered to be constant against temperature, while  $1/\tau_{cf}$  is Korringa-type relaxation between the  $f$  and conduction electrons and linear in temperature. As revealed in Fig. 4(a),  $1/T_1$  measured by  $^{29}\text{Si}$ -NMR of the isostructural non- $f$  compound  $\text{ThRu}_2\text{Si}_2$  [the broken line in Fig. 4(a) [13]] is much smaller than  $(1/T_1)_\perp$  for  $100 < T < 350$  K, namely  $(1/T_1)_c$  is negligible in this region. From these considerations, the temperature dependence of  $(1/T_1)_\perp$  for  $T > 100$  K is ascribed to that of  $(1/T_1)_f$  in which the predominant term shifts from  $1/\tau_{ff}$  for  $100 < T < 200$  K to  $1/\tau_{cf}$  for  $T > 200$  K.

For the relatively small  $(1/T_1)_\parallel$ , the  $(1/T_1)_c$  term should be responsible for a considerable part of the  $T_1$  relaxation. The  $(1/T_1)_\parallel$  data is well reproduced by a combination of the following two contributions:  $(1/T_1)_c$  (linear in temperature) and a temperature-independent term. The best fit gives  $(1/T_1)_c = 0.0136T$  [the dotted line in Fig. 4(a)], which is quite close to  $1/T_1$  for  $\text{ThRu}_2\text{Si}_2$  ( $1/T_1 = 0.0112T$  [13]). We will discuss the origin of the small constant term later.

On the other hand,  $(1/T_1)_\perp$  decreases below 100 K. One of the experimental reports supporting the itinerant picture of  $5f$  electrons just above  $T_{\text{HO}}$  in  $\text{URu}_2\text{Si}_2$  is the observation of  $(1/T_1)_i \propto T$  ( $i = \parallel$  and  $\perp$ ) behavior, reported in Ref. [5]. Therefore, in order to examine the temperature dependence of  $1/T_1$  in detail, we plot  $(1/T_1 T)_i$  vs  $T$  in Fig. 4(b). As decreasing temperature below 100 K,  $(1/T_1 T)_\perp$  deviates from the high-temperature Curie-like behavior [see the solid line in Fig. 4(b)] and shows a maximum around 40 K, instead of  $1/T_1 T \sim \text{const.}$  behavior. Note that such a series of temperature dependence of  $1/T_1 T$  for  $T > T_{\text{HO}}$  is often observed in heavy fermion compounds and intermediate valence compounds, which undergo a crossover from the localized state to the itinerant one with decreasing temperature [20]. Therefore the temperature of  $\sim 40$  K at which  $1/T_1 T$  exhibits the maximum is naturally interpreted as the characteristic temperature of the crossover. However, no observation of the  $1/T_1 T \sim \text{const.}$  behavior, characteristic of the Fermi liquid state, in  $\text{URu}_2\text{Si}_2$  reveals that the HO occurs before the Fermi liquid state is fully evolved. Thus the  $f$  state just above  $T_{\text{HO}}$  should be distinguished from the well itinerant system such as the so-called valence fluctuating state. In this context,  $K_\parallel$  presented in Fig. 3 also shows quite analogous behavior: the Curie Weiss behavior above 100 K and the maximum around 50 K. Thus, the present results consistently indicate that the HO occurs just below the characteristic temperature of the crossover between localized and itinerant regimes. Below  $T_{\text{HO}}$ , both  $(1/T_1)_i$  drop, followed by  $(1/T_1)_i \propto T$  behavior as shown in Fig. 4(a). This is in good agreement with previous reports [5,13].

From the  $T_1$  data, we extract information on anisotropic magnetic fluctuations in this compound. Nuclear spins are relaxed by the transverse components of hyperfine field fluctuations at the nuclear position, and  $(1/T_1)_\parallel$  and  $(1/T_1)_\perp$

are related to the dynamic susceptibilities  $\chi(q, \omega_0)$  for  $H \parallel c$  and  $H \perp c$ ,  $\chi_\parallel(q, \omega_0)$  and  $\chi_\perp(q, \omega_0)$ , respectively, as follows:

$$\left(\frac{1}{T_1}\right)_\parallel = \frac{2\gamma_n^2 k_B T}{(\gamma_e \hbar)^2} \sum_q \left[ A_\perp(q)^2 \frac{\text{Im}\chi_\perp(q, \omega_0)}{\omega_0} \right], \quad (1)$$

and

$$\left(\frac{1}{T_1}\right)_\perp = \frac{\gamma_n^2 k_B T}{(\gamma_e \hbar)^2} \sum_q \left[ A_\parallel(q)^2 \frac{\text{Im}\chi_\parallel(q, \omega_0)}{\omega_0} + A_\perp(q)^2 \frac{\text{Im}\chi_\perp(q, \omega_0)}{\omega_0} \right], \quad (2)$$

where  $\gamma_n$  and  $\gamma_e$  are the nuclear and electronic gyromagnetic ratios, respectively,  $\omega_0$  is the NMR frequency,  $\text{Im}\chi_i(q, \omega_0)$  is the imaginary part of  $\chi_i(q, \omega_0)$ , and  $A_i(q)$  is the hyperfine coupling constant. Using Eqs. (1) and (2) and the data of  $(1/T_1)_\parallel$  and  $(1/T_1)_\perp$ , we evaluate dynamic susceptibilities parallel and perpendicular to the  $c$  axis, defined as

$$S_\parallel \equiv \frac{\gamma_n^2 k_B}{(\gamma_e \hbar)^2} \sum_q \left[ A_\parallel(q)^2 \frac{\text{Im}\chi_\parallel(q, \omega_0)}{\omega_0} \right] \\ = \frac{1}{T} \left[ \left(\frac{1}{T_1}\right)_\perp - \frac{1}{2} \left(\frac{1}{T_1}\right)_\parallel \right],$$

and

$$S_\perp \equiv \frac{\gamma_n^2 k_B}{(\gamma_e \hbar)^2} \sum_q \left[ A_\perp(q)^2 \frac{\text{Im}\chi_\perp(q, \omega_0)}{\omega_0} \right] \\ = \frac{1}{2T} \left(\frac{1}{T_1}\right)_\parallel.$$

In Fig. 5(a), we plot  $S_i$  as a function of temperature. The significantly enhanced  $S_\parallel$  and the weakly temperature-dependent  $S_\perp$  reveal the Ising nature of not only the static magnetic properties but also the magnetic fluctuations in this compound. Figure 5(b) shows the temperature dependence of  $S_i T$ , which corresponds to decomposed  $1/T_1$  for each direction. Almost in the same manner as the discussion on the  $1/T_1$  data,  $S_\parallel T$  and  $S_\perp T$  for  $100 < T < 200$  K are well described as  $S_\parallel T = c_S$  and  $S_\perp T = a_S T + b_S$ , respectively, where  $c_S = 21.6 \text{ s}^{-1}$ ,  $a_S = 6.72 \times 10^{-3} \text{ s}^{-1} \text{ K}^{-1}$ , and  $b_S = 0.866 \text{ s}^{-1}$ .

By considering the existence of local moments above 100 K, the suppressions of  $S_i$  below  $\sim 40$  K indicate the decrease in the magnetic degrees of freedom through the crossover involved with the underlying Kondo screening. It is interesting to examine the  $q$  dependence in the suppressions of magnetic fluctuations. Since  $K_\parallel$  follows the Curie law for  $T > 100$  K and  $S_\parallel$  does the Curie-Weiss law for  $100 < T < 350$  K, we make the plot of  $S_\parallel^{-1}$  vs  $K_\parallel^{-1}$  with temperature as an implicit variable [see Fig. 6(a)]. As expected from their temperature dependences, the plot demonstrates a linear relation for  $50 < T < 210$  K. The slight upward deviation above 200 K corresponds to the downward deviation in  $S_\parallel T$  in the same temperature range from the constant [see Fig. 5(b)]. The most remarkable phenomenon in Fig. 6(a) is the rapid deviation from the linearity below 50 K. The direction of the departure from the linearity indicates that  $K_\parallel^{-1}$  increases more rapidly

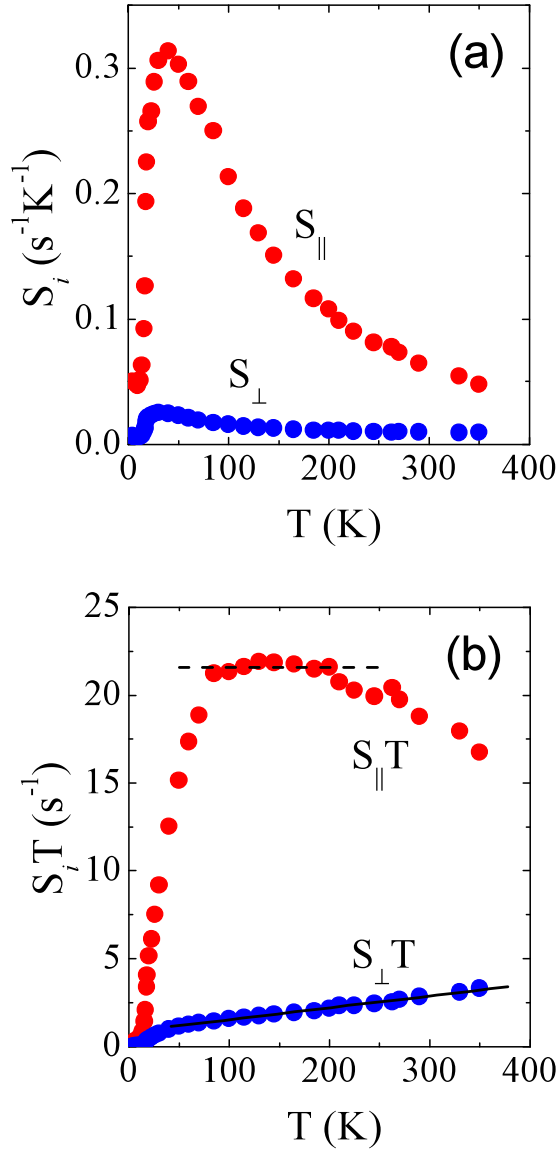


FIG. 5. Temperature dependences of (a)  $S_{\parallel}$  and  $S_{\perp}$  and (b)  $S_{\parallel}T$  and  $S_{\perp}T$ . The broken and solid lines are least-squares fits of  $S_{\parallel}T = c_S$  and  $S_{\perp}T = a_S T + b_S$ , respectively. See text for details.

than  $S_{\parallel}^{-1}$  does as temperature decreases below 50 K. One can also recognize this from the comparison of the temperature dependences of the two values shown in Fig. 6(b) where the axis of  $K_{\parallel}^{-1}$  is scaled so that the temperature linearity coincides with each other.  $K_{\parallel}^{-1}$  and  $S_{\parallel}^{-1}$  start to deviate upward from the temperature-linear relation below 100 K. However, the deviation of  $K_{\parallel}^{-1}$  is faster, and the difference between the two is pronounced for  $20 < T < 30$  K, just above  $T_{\text{HO}}$ . Therefore their temperature dependences cannot be scaled together by a linear relation.

For  $H \perp c$ , one of the possible explanations for the temperature dependence of  $\chi_{\perp}$  is given in Ref. [17]: it is accounted for in terms of crystalline electric field (CEF) scheme. Therefore we also attempt to reproduce  $K_{\perp}(T)$  above  $\sim 50$  K based on the CEF scheme, where we adopt the hyperfine coupling constant obtained from the  $K_{\perp}$  vs  $\chi_{\perp}$

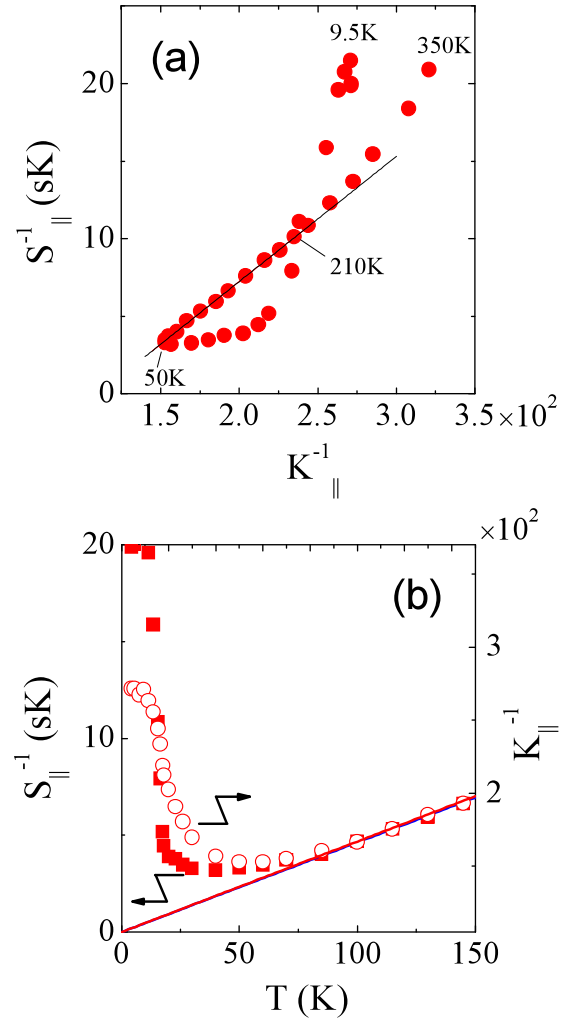


FIG. 6. (a) The plot of  $S_{\parallel}^{-1}$  vs  $K_{\parallel}^{-1}$  with temperature as an implicit variable. The solid line is a least-squares fit to the data. (b) Temperature dependences of the inverses of  $S_{\parallel}$  (left axis) and  $K_{\parallel}$  (right axis). The solid line represents a linear fit to the data, and the right vertical axis is scaled so that the two  $T$ -linear lines coincide with each other.

plot. The results are shown in the inset of Fig. 3(b) and Fig. 11 in Ref. [14], indicating that  $K_{\perp}$  and  $\chi_{\perp}$  for  $T > 50$  K are dominated by the Van Vleck term, while the Curie term is negligible. As shown in Fig. 5(b), we find the small temperature-independent term in  $S_{\perp}T$ . Although the origin of this constant term has not been clarified, one of the possible hypotheses is that there remain tiny magnetic fluctuations perpendicular to the  $c$  axis caused by the local moments. Indeed the temperature-independent term of  $S_{\perp}T$  is only  $\sim 4\%$  of that of  $S_{\parallel}T$ , seems to be consistent with the indication that the hyperfine field arising from the local moments vanishes for  $H \perp c$ , as far as analyzing  $K_{\perp}$ . Thus,  $K_{\perp}$  and  $S_{\perp}T$  are not sensitive to the feature of magnetic correlations at high temperatures.

The hyperfine coupling constant does not almost change across the crossover temperature [5,10], implying that the decreases in  $S_{\parallel}$  and  $K_{\parallel}$  below  $\sim 50$  K are ascribed to reductions in  $\chi(q, \omega_0)$ . One of the plausible interpretations of the more



rapid decrease in  $K_{\parallel}$  is that the suppression of magnetic fluctuations below the crossover temperature is not uniform, but dependent on  $q$ . As described in Eqs. (1) and (2),  $1/T_1$  reflects the  $q$  sum of  $\chi(q, \omega_0)$ , where  $\omega_0$  is regarded as  $\sim 0$  in the NMR measurement. On the other hand, the Knight shift is in proportion to  $q = 0$  component of  $\chi(q, 0)$ . According to these principles, the results in Figs. 6(a) and 6(b) suggest that the  $q = 0$  component of  $\chi(q, \omega)$  is suppressed more rapidly than  $q \neq 0$  components.

The difference demonstrated in Fig. 6 does not involve field-induced secondary components, since  $T_1$  does not show any field dependence between 0.5 and 6 T within experimental accuracy [see Fig. 10 in Ref. [14]]. From the existence of antiferromagnetic correlations just above  $T_{\text{HO}}$ , one may anticipate that the remaining correlations are concerned with the HO structure, although the HO does not involve magnetic ordering of dipole moments. In this context, the observed easy suppression of the  $q = 0$  correlation below the crossover temperature does not seem compatible with any ferro-type order in the HO phase. Unfortunately, we could not evaluate its specific  $q$  of the antiferromagnetic correlations only from the present study. We note that antiferromagnetic fluctuations are partially reduced at the Si site because of the effect of local crystallographic symmetry [13]. Therefore the real difference between  $S_{\parallel}$  and  $K_{\parallel}$  demonstrated in Fig. 6(a) can be enlarged.

It is interesting to compare the present results with indications by recent inelastic neutron scattering (INS) measurements. Regarding the observed remaining antiferromagnetic correlations just above  $T_{\text{HO}}$ , they seem consistent with the existence of magnetic excitations with commensurate and incommensurate wave numbers,  $q = (1\ 0\ 0)$  and  $(1 \pm 0.4\ 0\ 0)$ , respectively, revealed by INS measurements [21–23]. Moreover, the obtained crossover temperature  $\sim 100$  K between the localized to itinerant regimes is compatible with the

existence of itinerantlike spin excitations up to at least 10 meV [22].

Recently, the reductions in the susceptibility (therefore the Knight shift) and  $1/T_1 T$  below 25–30 K down to  $T_{\text{HO}}$  are explained in terms of the presence of a HO pseudogap: noncoherent order is formed in this temperature region [11, 24]. On the other hand, the recent INS studies [21–23] and the present results suggest the relationship between antiferromagnetic correlations with the HO. The latter implies that the magnetic correlations that survive below the crossover temperature are more directly associated with the HO than other correlations, which vanish in the same temperature region. The vanishing components may correspond to the pseudogap part. Thus, the present interpretation is incompatible with the pseudogap scenario. In order to obtain more information, NMR measurements at the Ru site might be useful.

In summary, we have precisely measured  $(1/T)_i$  and  $K_i$  ( $i = \parallel$  and  $\perp$ ) of  $\text{URu}_2\text{Si}_2$  up to 350 K by using a  $^{29}\text{Si}$ -enriched aligned powder sample. The temperature dependences of  $K_{\parallel}$  and  $(1/T_1)_{\perp}$  for  $T > 100$  K are well accounted for by the localized regime of 5  $f$  electrons, while  $(1/T_1 T)_{\perp}$  exhibits a peak around 40 K without showing  $1/T_1 T \sim \text{const.}$  behavior characteristic of the Fermi liquid state above  $T_{\text{HO}}$ . These results naturally indicate that  $\text{URu}_2\text{Si}_2$  undergoes a crossover between localized and itinerant regimes and that the HO occurs in the crossover region. We also extracted magnetic fluctuation components parallel and perpendicular to the  $c$  axis and consequently presented a new aspect of the persistence of antiferromagnetic correlations down to  $T_{\text{HO}}$ .

We thank Y. Kohori, H. Amitsuka, H. Tou, K. Ishida, Y. Hasegawa, and H. Kusunose for valuable discussions. This work was partially supported by JSPS KAKENHI (Grants No. 24540349 and No. 16K05457).

- 
- [1] For a review, see J. A. Mydosh and P. M. Oppenher, *Rev. Mod. Phys.* **83**, 1301 (2011).
  - [2] T. T. M. Palstra, A. A. Menovsky, J. van den Berg, A. J. Dirkmaat, P. H. Kes, G. J. Nieuwenhuys, and J. A. Mydosh, *Phys. Rev. Lett.* **55**, 2727 (1985).
  - [3] W. Schlitz, J. Baumann, B. Pollit, U. Rauchschwalbe, H. M. Mayer, U. Ahlheim, and C. D. Bredl, *Z. Phys. B*, **62**, 171 (1986).
  - [4] M. B. Maple, J. W. Chen, Y. Dalichaouch, T. Kohara, C. Rossel, M. S. Torikachvili, M. W. McElfresh, and J. D. Thompson, *Phys. Rev. Lett.* **56**, 185 (1986).
  - [5] Y. Kohori, K. Matsuda, and T. Kohara, *J. Phys. Soc. Jpn.* **65**, 1083 (1996).
  - [6] K. Matsuda, Y. Kohori, and T. Kohara, *J. Phys. Soc. Jpn.* **65**, 679 (1996).
  - [7] K. Matsuda, Y. Kohori, T. Kohara, K. Kuwahara, and H. Amitsuka, *Phys. Rev. Lett.* **87**, 087203 (2001).
  - [8] O. O. Bernal, C. Rodrigues, A. Martinez, H. G. Lukefahr, D. E. MacLaughlin, A. A. Menovsky, and J. A. Mydosh, *Phys. Rev. Lett.* **87**, 196402 (2001).
  - [9] S. Takagi, S. Ishihara, M. Yokoyama, and H. Amitsuka, *J. Phys. Soc. Jpn.* **81**, 114710 (2012).
  - [10] S. Kambe, Y. Tokunaga, H. Sakai, T. D. Matsuda, Y. Haga, Z. Fisk, and R. E. Walstedt, *Phys. Rev. Lett.* **110**, 246406 (2013).
  - [11] K. R. Shirer, J. T. Haraldsen, A. P. Dioguardi, J. Crocker, N. apRoberts-Warren, A. C. Shockley, C.-H. Lin, D. M. Nisnon, J. C. Cooley, M. Janoschek, K. Huang, N. Kanchanavatee, M. B. Maple, M. J. Graf, A. V. Balatsky, and N. J. Curro, *Phys. Rev. B*, **88**, 094436 (2013).
  - [12] T. Mito, M. Hattori, G. Motoyama, Y. Sakai, T. Koyama, K. Ueda, T. Kohara, M. Yokoyama, and H. Amitsuka, *J. Phys. Soc. Jpn.* **82**, 123704 (2013).
  - [13] N. Emi, R. Hamabata, D. Nakayama, T. Miki, T. Koyama, K. Ueda, T. Mito, Y. Kohori, Y. Matsumoto, Y. Haga, E. Yamamoto, and Z. Fisk, *J. Phys. Soc. Jpn.* **84**, 063702 (2015).
  - [14] See Supplemental Material at <http://link.aps.org/supplemental/10.1103/PhysRevB.96.195113> for details, which includes Refs. [15, 16].
  - [15] H. G. Lukefahr, J. K. Collins, E. Camacho, C. Yeager, D. E. MacLaughlin, A. Myers, and O. O. Bernal, *Rev. Sci. Instrum.* **67**, 3642 (1996).
  - [16] M. Benakki, A. Qachaou, and P. Panissod, *J. Magn. Magn. Mater.* **73**, 141 (1988).

- [17] A. Galatanu, Y. Haga, T. D. Matsuda, S. Ikeda, E. Yamamoto, D. Aoki, T. Takeuchi, and Y. Onuki, *J. Phys. Soc. Jpn.* **74**, 1582 (2005).
- [18] D. E. MacLaughlin, O. Penna, and M. Lysak, *Phys. Rev. B.* **23**, 1039 (1981).
- [19] For example, M. Matsumura, N. Tomita, S. Tanimoto, Y. Kawamura, R. Kobayashi, H. Kato, T. Nishioka, H. Tanida, and M. Sera, *J. Phys. Soc. Jpn.* **82**, 023702 (2013).
- [20] N. Tsujii, K. Yoshimura, and K. Kosuge, *Phys. Rev. B.* **59**, 11813 (1999).
- [21] C. Broholm, H. Lin, P. T. Matthews, T. E. Mason, W. J. L. Buyers, M. F. Collins, A. A. Menovsky, J. A. Mydosh, and J. K. Kjems, *Phys. Rev. B.* **43**, 12809 (1991).
- [22] C. R. Wiebe, J. A. Janik, G. J. Macdougall, G. M. Luke, J. D. Garrett, H. D. Zhou, Y.-J. Jo, L. Balicas, Y. Qiu, J. R. D. Copley, Z. Yamani, and W. J. L. Buyers, *Nature Phys.* **3**, 96 (2007).
- [23] F. Bourdarot, E. Hassinger, S. Raymond, D. Aoki, V. Taufour, L.-P. Regnault, and J. Flouquet, *J. Phys. Soc. Jpn.* **79**, 064719 (2010).
- [24] J. T. Haraldsen, Y. Dubi, N. J. Curro, and A. V. Balatsky, *Phys. Rev. B.* **84**, 214410 (2011).